Received: 15 April 2022 | Revised: 2 December 2022 | Accepted: 6 December 2022

DOI: 10.1002/nag.3480

RESEARCH ARTICLE

WILEY

A beam on elastic foundation method for predicting deflection of braced excavations considering uncertainties

Cong Tang | **Shu-Yu He** | **Wan-Huan Zhou**

State Key Laboratory of Internet of Things for Smart City and Department of Civil and Environmental Engineering, University of Macau, Macau SAR, China

Correspondence
Wan-Huan Zhou, State Key Laboratory of Internet of Things for Smart City and Department of Civil and Environmental Engineering, University of Macau, Macau SAR, China.
Email: hannahzhou@um.edu.mo

Funding information
Science and Technology Development Fund, Macau SAR, Grant/Award Number: SKL-IOTSC(UM)-2021-2023; National Natural Science Foundation of China, Grant/Award Number: 52022001; Science and Technology Program of Guangdong Province, Grant/Award Number: 2021A0505080009; Research Committee of University of Macau, Grant/Award Number: MYRG2018-00173-FST; Science and Technology Development Fund, Macau SAR, Grant/Award Number: 0057/2020/AGJ

Abstract

Predicting wall deflection is important to provide a critical reference to evaluate the current construction conditions and prevent potential damage risks of adjacent facilities during excavations. This paper presents a combination of a beam on elastic foundation model (BEFM) and the Bayesian framework to realize effective probabilistic predictions of wall deflection at various depths in braced excavations. First, a finite element solving algorithm to calculate wall deflection for the BEFM is developed and incorporated into the Bayesian framework. Next, the most suitable distribution pattern for soil resistance and an appropriate set of uncertain parameters in the BEFM are determined through the application of the Bayesian model selection technique. Meanwhile, the uncertain parameters are updated. A prediction is then made using the optimal model and corresponding posterior probability distributions of the updated parameters at each stage. The parameter updating and prediction process are repeated as additional field observations become available during construction. The performance of the proposed method is examined using a field case study. The results show that this method provides a satisfactory approach to predict both the magnitudes and profile of deflection when considering uncertainties. Additionally, comparisons with a Bayesian updating framework using a surrogate model (i.e., the KJHH model) indicate higher updating efficiency of the developed method.

KEYWORDS
Bayesian probabilistic method, beam on elastic foundation, braced excavations, uncertainty, wall deflection

1 | INTRODUCTION

Braced excavations play an important role in urban constructions. However, ground movement induced by braced excavations may cause damage to adjacent infrastructures, such as buildings, pipelines, and tunnels.[1-3] To ensure the serviceability safety of braced excavations, the maximum wall deflection should not exceed a tolerable limit.[4-6] For example, tolerable limits are set to 0.14%H–0.70%H (H is the excavation depth) to satisfy different

requirements of environmental protection based on local engineering experience in Shanghai, China.[4] Additionally, abnormal deflection patterns of wall deflection should be avoided to prevent possible failures.[7] For instance, a kick-out failure may occur when basal strata cannot provide sufficient constraints to lateral wall deflection below the excavation base.[7,8] Accordingly, information from the wall deflection provides a critical reference to evaluate current construction conditions in excavation projects, based on which some adjustments to the construction activities can be made to prevent potential damage risks.[6,9]

The finite element method (FEM) and simplified model are popular ways to assess wall deflection in braced excavations.[5,10] However, the estimated results may deviate significantly from observations due to the high degree of uncertainties from soil properties, model error, construction variability, etc., in braced excavations.[11-14] An effective solution is to combine the prediction model with a back analysis framework to enhance the prediction accuracy by extracting knowledge from field observations. There are several methods for the back analysis of geotechnical problems, such as the multi-objective optimization,[15] differential evolution algorithm,[10] and Bayesian method.[13,14,16] Among them, the Bayesian method can update probability density functions (PDFs) of the input parameters based on field observations, whereas most other methods regard the soil parameters as constants and can only perform deterministic analyses.[14,16] In other words, uncertainty in the input parameters can be quantified using the Bayesian method. This uncertainty quantification is meaningful as variations in the input parameters and the computed responses are fully characterized.[16] Additionally, a reliability assessment or a reliability-based design optimization can be further performed as the PDFs of deflection can be obtained.[13,17]

This Bayesian probabilistic framework had been applied in various geotechnical structures, including braced excavations, to analyze wall deflection.[14,16-20] Previous research indicated that a direct combination of the uncertainty analysis framework with the FEM could be highly time-consuming and computationally intensive because numerous computations rounds were required.[17] Alternatively, several surrogate models were proposed for predictions based on a fitting analysis of the database derived from a series of well-calibrated finite element analyses or high-quality field observations under similar geological conditions. These models were usually represented by simple polynomials, which allowed a more efficient deflection assessment even if users had no background in FEM. Accordingly, it is easy to combine probabilistic theory with these models to realize uncertainty analysis. For example, Juang et al.[16] proposed a Bayesian framework to update soil parameters in the KJHH model using field observations, and more accurate predictions of the maximum wall deflection and maximum ground settlement were obtained. Wu et al.[13] proposed a novel procedure to update the probability distributions of the maximum wall deflection by quantifying the estimation errors between the actual and estimated values. They adopted a regression model derived from the field data from 22 case histories in Taipei as the prediction model. Qi and Zhou[14] obtained an efficient model to predict wall deflection using the response surface method, which was combined with a Bayesian back-analysis procedure to quantify uncertainty in the soil parameters. These surrogate models were proved to be good representations of the fine finite element solutions or empirical statistical relationships of excavations-induced deflection. However, the sole output of these surrogate models is generally the maximum deflection, and the deflection profile cannot be obtained. This also means that the model can only be updated using information from the maximum deflection at each stage, which limits the updating efficiency. Additionally, significant efforts may be still required to retrain a new surrogate model when geotechnical conditions differ from what the surrogate model was built on.[48]

To address these issues, this paper investigates the potential of combining a beam on elastic foundation model (BEFM) and the Bayesian probabilistic framework. The advantages of this method are given as: (1) deflection at any point along the depth (i.e., deflection magnitudes and profile) and associated uncertainties can be assessed; (2) all the deflection observations can be used for updating to improve efficiency; and (3) there is no need to cost additional time and computational resources to train a new surrogate model when the existing surrogate models are not applicable. In detail, a computer code of the finite element solving algorithm is developed to compute the wall deflection in the BEFM. This algorithm is then coupled with a Bayesian framework to conduct parameter updating and uncertainty quantification. The model selection technique is used to determine the most suitable distribution pattern of the soil resistance and an appropriate set of uncertain parameters in the BEFM at the early stage. Then, both the magnitudes and profile of wall deflection are predicted using the most suitable model and its updated parameters.

The remainder of this paper is organized as follows. First, the basic principles of the BEFM and the Bayesian updating framework are introduced. Then, a field excavation case is adopted to demonstrate the method's effectiveness, where comparisons between the proposed method and other methods are conducted. Finally, the conclusions are presented.

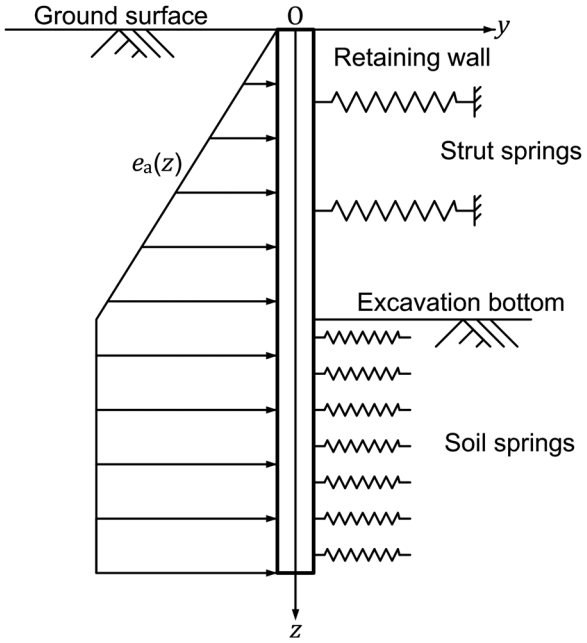

FIGURE 1 Schematic diagram of the BEFM for retaining wall analysis

2 | METHODOLOGY

2.1 | Beam on elastic foundation model

2.1.1 | Basic principles

The basic idea of the BEFM is to simulate soil-structure interactions through a series of individual springs.[25,49] The soil spring constant, also referred to as the coefficient of subgrade reaction, is the ratio of the stress to the displacement based on the assumptions of the Winkler model.[21-24] Applying this method to a braced excavation involves three fundamental assumptions[22,25]: (1) the retaining wall is simulated as a vertical continuous beam of unit width under plane strain conditions; (2) struts are simplified as spring supports, with the soil below the excavation bottom modeled as soil springs; (3) the soil pressure acting on the outside of the wall is calculated using the Rankine active earth pressure theory above the excavation bottom but remains constant below. As a result, the soil pressure in the active zone is regarded as a load, with the soil springs and struts springs representing the passive soil resistance and strut resistance, respectively. As excavation proceeds, unloading induced by excavation creates an imbalance of the force between the two sides of the wall and causes it to deform. The pressure and resistance will constantly adjust to ensure the entire retaining structure is in a state of dynamic equilibrium. Figure 1 shows the schematic diagram of the BEFM for the retaining wall analysis. The governing equation for wall deformation can be expressed as[21-24]:

$$EI\frac{d^4y}{dz^4} - e_a(z)\ b_0 = 0\ (0 \le z \le h_r)$$

$$EI\frac{d^4y}{dz^4} + cf \cdot y \cdot b_0 - e_a(z)\ b_0 = 0\ (z \ge h_r) \tag{1}$$

where b_0 is the calculation width, usually set to 1 m (i.e., unit width) for the retaining wall, and E and I are Young's modulus and area moment of inertia of the wall, respectively. Thus, EI denotes the bending stiffness of the wall per unit width. y is the lateral wall deflection, z is the depth below the ground surface, h_r is the excavation depth at the rth stage, $e_a(z)$ is the Rankine active earth pressure at depth z, and cf is the soil spring constant.

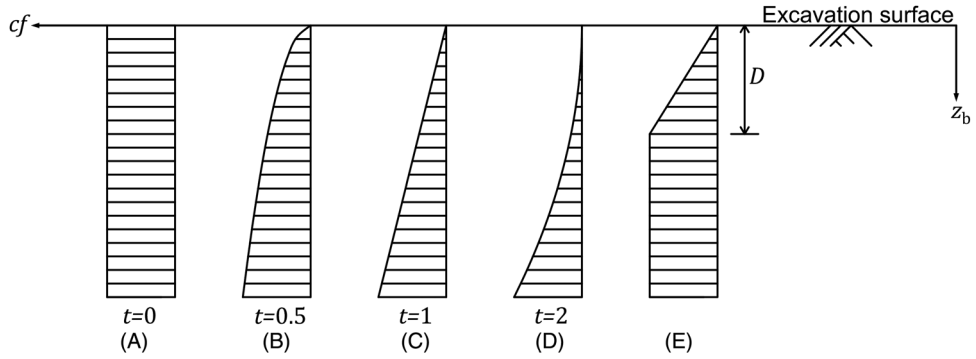

FIGURE 2 Five distribution patterns of the soil spring constant along the depth

In general, variations of the soil spring constant (soil resistance) along the depth are assumed to obey the equation[22,26]:

$$cf = g(z_b) = A_0 + k_s(z_b)^t \tag{2}$$

where k_s is the scale factor of the soil spring constant, z_b is the depth below the excavation bottom (i.e., $z_b = z - h_r$), A_0 is the soil spring constant at the excavation bottom for each stage (normally assumed to be zero), and t is an exponent whose value is set to 0, 0.5, 1, or 2, corresponding to four different distribution patterns of the soil spring constant, as shown in Figure 2A–D. An additional distribution pattern is a combination of the cases $t = 0$ and $t = 1$ (Figure 2E). In this pattern, D is the disturbance depth of the soil below the bottom induced by staged excavation, generally assumed to be 3–5 m.[24] Notably, the pattern $t = 1$ (Figure 2C) is the most common case used for engineering calculations; however, this pattern may not always be the most suitable pattern for different excavations. Thus, it would be meaningful if the most suitable pattern can be selected before implementing formal computations.

The scale factor suffers from significant randomness and uncertainty because it is easily affected by many factors, such as soil properties, wall deformation, and disturbances to the surrounding soil during excavations. This value is generally acquired through local experience or back analysis using field observations.[22-24,27] Theoretically, different scale factors should be assigned to different layers, but owing to the uneven spatial distribution of soil layers and the limited number of drill holes on site, actual soil stratification is not completely clear.[28] In addition, if multiple scale factors are used, too many uncertain parameters will be introduced into the BEFM, which would require more observations and computational effort.[16] Accordingly, an equivalent scale factor k_{sr} is proposed to signify the effect of soil resistance along the wall depth. Briefly, k_{sr} is referred to as the soil resistance factor in subsequent sections.

The soil properties' inherent variability and measurement error indicate that the Rankine active earth pressure $e_a(z)$ should be treated as a random variable.[11] Similarly, due to the limited knowledge of soil stratification and to alleviate computational burdens, the soil pressure factor k_a is introduced to represent the effect of soil pressure, computed by equating the area of the Rankine active earth pressure along the depth to that of the simplified triangle-distributed pressure (Figure 1). This equivalence ensures that the resultant earth pressure acting on the retaining wall remains unchanged. Thus $e_a(z)$ is expressed as:

$$e_a(z) = \begin{cases} k_a z & (0 \le z \le h_r) \\ k_a h_r & (z \ge h_r) \end{cases} \tag{3}$$

The struts (or slab floors) are regarded as elastic supports and bear only axial forces. The reactions of struts are computed by[23,24]:

$$T^{(u)} = \left(K_{strut}^{(u)}\left(y_{now}^{(u)} - y_0^{(u)}\right) - P_{pre}\right) b_0 \tag{4}$$

where $K_{strut}^{(u)}$ is the axial stiffness of the uth strut, $y_{now}^{(u)}$ is the current deflection at the depth of the uth strut, $y_0^{(u)}$ is the initial deflection at the depth of the uth strut before the strut has been installed, and P_{pre} is the preload of steel struts per calculation width.

TABLE 1 The 10 candidate model classes and their parameters

Model class number	Distribution patterns of soil spring constant	Uncertain parameters vector θ
1	$D1$ ($t = 0$)	$[k_{sr}, k_a, \sigma_\varepsilon]^T$
2	$D2$ ($t = 0.5$)	$[k_{sr}, k_a, \sigma_\varepsilon]^T$
3	$D3$ ($t = 1$)	$[k_{sr}, k_a, \sigma_\varepsilon]^T$
4	$D4$ ($t = 2$)	$[k_{sr}, k_a, \sigma_\varepsilon]^T$
5	$D5$ ($t = 0$ or $t = 1$)	$[k_{sr}, k_a, \sigma_\varepsilon]^T$
6	$D1$ ($t = 0$)	$[k_{sr}, k_a, K_{strut}, \sigma_\varepsilon]^T$
7	$D2$ ($t = 0.5$)	$[k_{sr}, k_a, K_{strut}, \sigma_\varepsilon]^T$
8	$D3$ ($t = 1$)	$[k_{sr}, k_a, K_{strut}, \sigma_\varepsilon]^T$
9	$D4$ ($t = 2$)	$[k_{sr}, k_a, K_{strut}, \sigma_\varepsilon]^T$
10	$D5$ ($t = 0$ or $t = 1$)	$[k_{sr}, k_a, K_{strut}, \sigma_\varepsilon]^T$

The axial stiffness of struts is computed by[23]:

$$K_{strut} = \frac{\alpha_R b_0 E_{strut} A_{strut}}{\lambda_0 S_{strut} L_{strut}} \tag{5}$$

where α_R is the relaxation coefficient of struts, $\alpha_R = 1.0$ is for concrete struts (slab floors) or steel struts with preload, and $\alpha_R = 0.8$–1.0 is for steel struts without preload. E_{strut}, A_{strut}, S_{strut}, and L_{strut} are Young's modulus, equivalent cross-section area, average horizontal spacing, and length of a strut, respectively. λ_0 is the adjustment factor of the fixed point to consider the unsymmetrical load effect from two sides of the excavation. For symmetrical excavations, λ_0 is set to 0.5. If floor slabs are used as supports in an excavation constructed using the top-down method, S_{strut} should be set to 1 m.

As illustrated by Equation (5), the axial stiffness of struts can be affected by various factors such as load conditions, strut horizontal spacings, preload, dimensions, and strength performance of the used materials. Furthermore, the axial stiffness of struts is also susceptible to construction quality as installation errors can affect their support performance.[40] In a word, the axial stiffness of struts is a comprehensive parameter herein and may involve large uncertainties in practice. Although structural parameters are generally assumed to be less variable than soil parameters and are considered constants in most geotechnical problems, treating the strut axial stiffness as a variable may be more appropriate in some cases.

According to Juang et al.,[29] a model with more uncertain parameters may yield a more effective result from the perspective of model fidelity. However, the increase in the number of uncertain parameters could make it more difficult to accurately characterize these parameters given the same amount of observed data. Besides, parameters' uncertainties tend to increase, especially when limited observations are available. Conversely, a model that has fewer uncertain parameters is more robust against uncertainties, but its predictive ability may not be as good as a complex model's. Whether the axial stiffness of struts should be taken as an uncertain parameter is worth serious consideration, and the Bayesian model selection technique can help in making this decision. Combined with five different distribution patterns of the soil spring constant, a total of 10 candidate model classes and associated uncertain parameters are listed in Table 1, with $D1 - D5$ denoting distribution patterns (A)–(E), respectively. σ_ε signifies the standard deviation (SD) of the prediction error, as discussed in Section 3.

2.1.2 | Finite element solving algorithm

The finite element solving algorithm based on Euler–Bernoulli beam theory is adopted to compute deflection in the BEFM. The algorithm can be enacted through the following steps[22,25,30]:

1. The retaining wall is regarded as a beam on the elastic foundation and needs to be partitioned into beam elements. The length of the beam elements h should be selected by considering some important factors, such as the excavation depth and strut location.

2. A set of interpolation functions ϕ^n is used to establish the matrix equation, which is expressed in terms of the local coordinate $\bar{z} = z - z_n$:

$$\phi_1^n = 1 - 3\left(\frac{\bar{z}}{h_n}\right)^2 + 2\left(\frac{\bar{z}}{h_n}\right)^3, \quad \phi_2^n = -\bar{z}\left(1 - \frac{\bar{z}}{h_n}\right)^2,$$

$$\phi_3^n = 3\left(\frac{\bar{z}}{h_n}\right)^2 - 2\left(\frac{\bar{z}}{h_n}\right)^3, \quad \phi_4^n = -\bar{z}\left[\left(\frac{\bar{z}}{h_n}\right)^2 - \frac{\bar{z}}{h_n}\right] \tag{6}$$

where n denotes the index of the beam element.

According to the principle of virtual work, the element matrix equation is obtained as:

$$\sum_{j=1}^{4} K_{ij}^n \Delta_j^n - F_i^n = 0 \text{ or } [K^n]\{\Delta^n\} = \{F^n\} \tag{7}$$

with

$$K_{ij}^n = \int_0^{h_n} (EI \frac{d^2\phi_i^n}{d\bar{z}^2} \frac{d^2\phi_j^n}{d\bar{z}^2} + cf\phi_i^n\phi_j^n) d\bar{z} \tag{8}$$

$$F_i^n = \int_0^{h_n} \phi_i^n e_a(\bar{z})\, d\bar{z} + Q_i^n \tag{9}$$

where i and j both denote the index of the interpolation function (i =1,2,3,4; and j =1,2,3,4). $[K^n]$, $\{\Delta^n\}$, and $\{F^n\}$ are, respectively, the stiffness matrix, vector of generalized displacements, and vector of generalized forces of the nth beam element. Q^n is the external bending moment, or the point force acting on the nodes of the nth beam element, which is usually considered as a strut reaction T.

3. The global matrix equation is obtained by assembling all the element matrices based on the node's force equilibrium and deformation compatibility conditions. The deflection of the retaining wall at each node is then calculated through matrix operations.

2.2 | Bayesian probabilistic framework

The goal of the Bayesian probabilistic framework is to select the most plausible model class from a family of competitive model classes $\{M^{(m)} : m = 1, \ldots, N_m\}$ based on their measurements, whereas the key uncertain parameter vector $\boldsymbol{\theta}$ of the model class $M^{(m)}$ is effectively identified.[31] $Y = [y_1, y_2, \ldots, y_N]$ denotes the vector of observed deflection at different depths along the retaining wall, and $h(\boldsymbol{\theta}_m|M^{(m)}) = [h_1(\boldsymbol{\theta}_m|M^{(m)}), h_2(\boldsymbol{\theta}_m|M^{(m)}), \cdots, h_N(\boldsymbol{\theta}_m|M^{(m)})]$ represents the vector of predicted deflection at the corresponding depths. The observations and model predictions are assumed to satisfy the equation[12,31,32,47]:

$$Y = h(\boldsymbol{\theta}_m|M^{(m)}) + \varepsilon \tag{10}$$

where N denotes the number of observed points. $\varepsilon = [\varepsilon_1, \varepsilon_2, \ldots, \varepsilon_N]$ is an N-vector of the prediction errors, where ε_n ($n = 1, 2, \ldots, N$) is assumed to be a zero-mean Gaussian random variable with an SD of σ_ε. The σ_ε is another unknown parameter beyond the model parameters $\boldsymbol{\theta}_m$. Accordingly, the uncertain parameter vector $\boldsymbol{\theta}$ includes the model parameters and the prediction error SD σ_ε, that is, $\boldsymbol{\theta} = [\boldsymbol{\theta}_m^T, \boldsymbol{\sigma}_\varepsilon]^T$.

According to Bayes's theorem, the posterior PDF of $\boldsymbol{\theta}$ in the model class $M^{(m)}$ can be written as[33]:

$$f\left(\boldsymbol{\theta}|\mathbf{Y},\ \mathbf{M^{(m)}}\right)=\frac{f\left(\boldsymbol{\theta}|\mathbf{M^{(m)}}\right)f\left(Y|\boldsymbol{\theta},\ \mathbf{M^{(m)}}\right)}{f\left(Y|M^{(m)}\right)} \tag{11}$$

where $f(\boldsymbol{\theta}|\mathbf{M^{(m)}})$ is the prior PDF of $\boldsymbol{\theta}$ and representing the user's judgment or previous knowledge before the data Y are observed. $f(Y|M^{(m)})=\int f(\boldsymbol{\theta}|\mathbf{M^{(m)}})\mathbf{f}(\mathbf{Y}|\boldsymbol{\theta},\ \mathbf{M^{(m)}})\mathbf{d}\boldsymbol{\theta}$ is the evidence for the model class $M^{(m)}$ provided by the data Y, which is a key component in model selection. $f(Y|\boldsymbol{\theta},\ \mathbf{M^{(m)}})$ is the likelihood function that expresses the level of data fitting.

If the prediction errors of the measured data are statistically independent, then the likelihood function can be computed as[31,32]:

$$f\left(Y|\boldsymbol{\theta},\ \mathbf{M^{(m)}}\right)=\left(2\pi\sigma_{\varepsilon}^{2}\right)^{-\frac{N}{2}}\exp\left\{-\frac{\sum_{n=1}^{N}\left[y_n-h_n\left(\boldsymbol{\theta}_{\mathrm{m}}|M^{(m)}\right)\right]^2}{2\sigma_{\varepsilon}^{2}}\right\} \tag{12}$$

After the prior PDF and likelihood function are defined, the posterior PDF of $\boldsymbol{\theta}$ can be obtained by Equation ([11]).

Once the evidence of each candidate model has been computed, the most suitable model class can be selected based on the posterior probability/plausibility of the candidate model classes conditional on the measurement Y. The posterior probability is given by[31-33]:

$$P(M^{(m)}|Y)=\frac{P\left(M^{(m)}\right)f\left(Y|M^{(m)}\right)}{\sum_{m=1}^{N_m}\left[P\left(M^{(m)}\right)f\left(Y|M^{(m)}\right)\right]} \tag{13}$$

where N_m is the number of candidate model classes. $\sum_{m=1}^{N_m}[P(M^{(m)})f(Y|M^{(m)})]$ is a normalizing constant, and $P(M^{(m)})$ expresses the user's judgment on the initial plausibility of the model classes with $\sum_{m=1}^{N_m}P(M^{(m)})=1$. In general, a uniform prior plausibility is assumed, that is, $P(M^{(m)})=1/N_m$, indicating that the model class with the largest evidence $f(Y|M^{(m)})$ will be the most suitable model.[31]

In this study, the differential evolution transitional Markov chain Monte Carlo (DE-TMCMC) algorithm proposed by Jin et al.[35,36] is used to perform model class selection and parameter updating. The details of this algorithm are given in Appendix A.

2.3 | Flowchart of the proposed method

The flowchart of the proposed method is illustrated in Figure 3. First, the necessary engineering data are collected, and the prediction model is established for braced excavations based on the proposed BEFM and the corresponding finite element solving algorithm. Second, a total of 10 candidate model classes and their corresponding prior PDFs of uncertain parameters are determined (Table 1). Once the observations of the early stage are available, model selection and parameter updating are performed simultaneously, after which, predictions are made for subsequent stages using the most suitable model. As excavation progresses, parameter updating and deflection predictions are performed repeatedly until the final excavation depth is reached.

3 | FIELD CASE STUDY OF TNEC EXCAVATION

The Taipei National Enterprise Center (TNEC) excavation is adopted as a field case study to illustrate the effectiveness of the proposed method. The TNEC excavation is a multi-propped deep excavation, with five story buildings in the vicinity. Figure 4 presents the soil profile and cross-section of the TNEC excavation. The excavation was performed using the

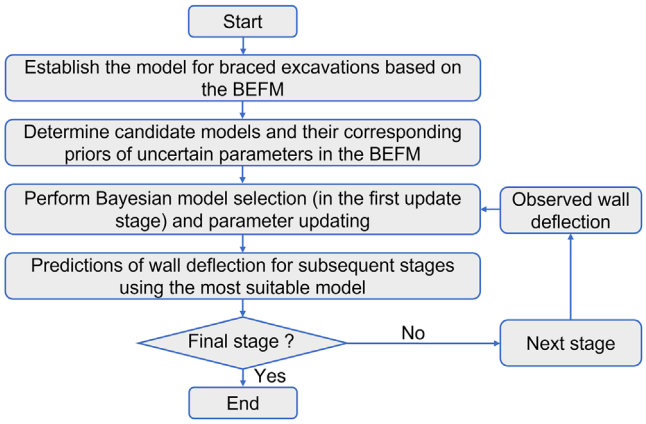

FIGURE 3 Flowchart of the proposed method

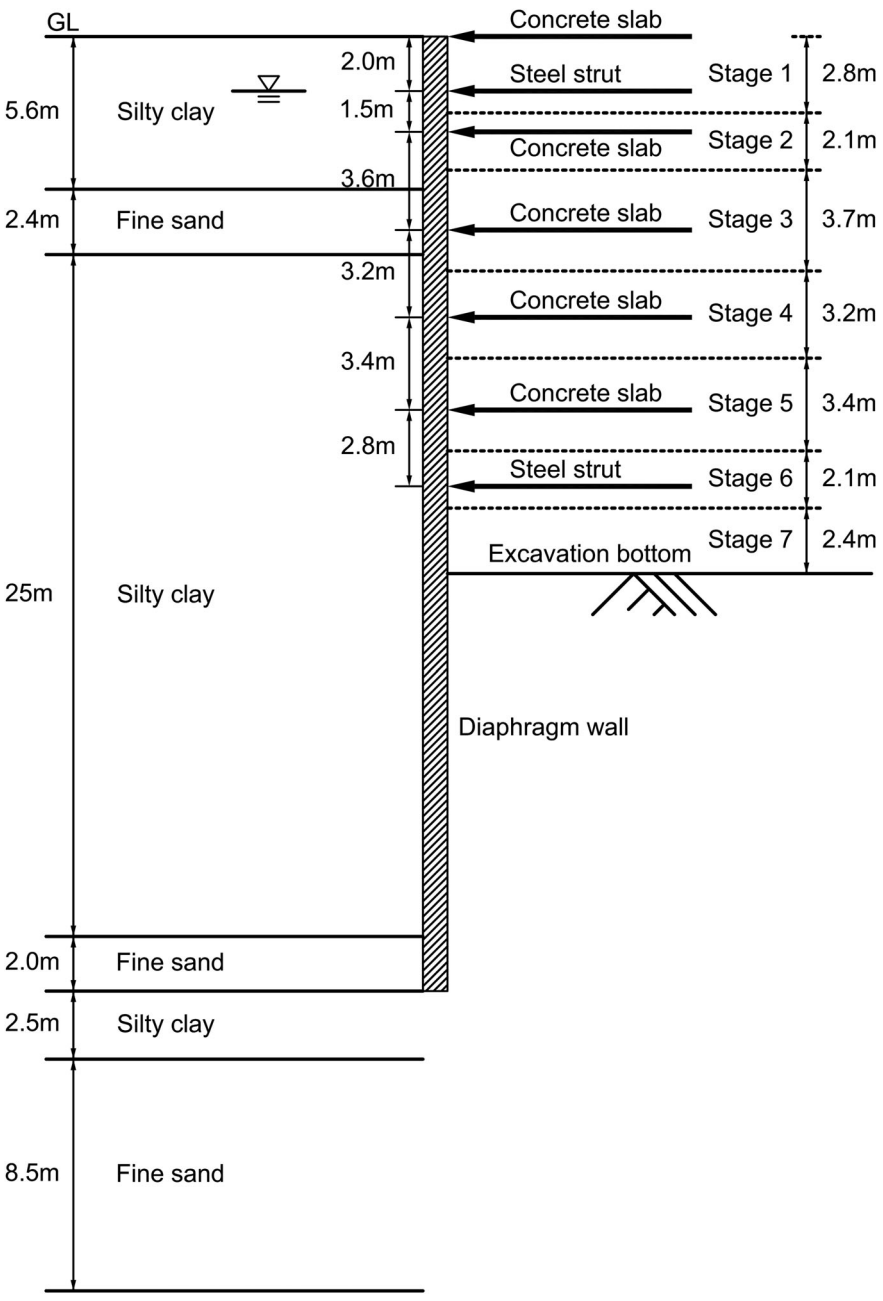

FIGURE 4 Soil profile and cross-section of the TNEC excavation

TABLE 2 Summary of prior PDFs

Parameters	Prior PDFs			
	Uniform distribution		Lognormal distribution	
	Lower bound	Upper bound	Mean	COVs
σ_ε (mm)	0	2.00×10^1	–	–
k_{sr} (kN/m^u)	0	2.00×10^4	–	–
k_a (kN/m^3)	–	–	1.17×10^1	0.30
K_{strut} (kN/m)	–	–	1.53×10^5	0.30

Note: The units of k_{sr} depend on the distribution patterns of the soil spring constant, the values of u can be 3, 3.5, 4, or 5.

top-down method in seven stages with a maximum excavation depth of 19.7 m, and it was supported by the 0.9-m-thick diaphragm wall and seven levels of struts. Most struts were cast concrete slabs, and the remaining were steel pipes with preloads. Of note, the first steel strut was demolished and substituted with a concrete slab at the ground surface before excavation to 8.5 m. The subsoil at the TNEC site consisted of six alternating silty clay and fine sand layers overlying a hard stratum layer of dense gravel soil. Most excavation stages were in silty clay. Additionally, the groundwater table level was 2.0 m below the ground surface before excavation. As the TNEC excavation had well-documented observations of good quality, it had been adopted as an illustrated example in several previous studies.[10,41,42] Additional details about the TNEC excavation can be found in Ou et al.[1,39]

3.1 | Parameter setting

The prior PDFs should be determined before the calculations. As there is no reliable way to determine the exact values of the soil resistance factor k_{sr} and prediction error SD σ_ε, these two parameters are assumed to obey uninformative distributions, that is, uniform distributions. Additionally, the prior PDFs of the soil pressure factor k_a and strut axial stiffness K_{strut} are taken as lognormal distributions to avoid possible negative values in the model parameters.[16,17,38] As described previously, the prior mean value of k_a is computed based on the Rankine active earth pressure theory, whereas that of K_{strut} is calculated from Equation (5). The coefficients of variation (COVs) for these two prior PDFs are set to 0.30 based on the soil test results and engineering experience.[11,14,22-24] Table 2 summarizes the prior PDFs used in this case. Additionally, the bending stiffness of the diaphragm wall (EI) is calculated as 1.28×10^6 kN·m^2, and the preload (P_{pre}) of the second steel strut is 392 kN/m per unit width.[39]

In the early stages (first or second stage) of excavation, the updating procedure might be meaningless, because the associated deflection data usually suffer from greater relative measurement errors, and the deformed profile of the wall inevitably changes from a cantilever to a concave-type profile.[14,16] Thus, the updating begins from stage 3 in this case. Additionally, sufficient samples are required to ensure an effective MCMC sampling. Herein, the Gelman-Rubin diagnostic is performed to check the sample convergence.[43] If the calculated potential scale reduction factor (PSRF), which is defined as the ratio of the within-chain and between-chain variances of uncertain variables, is smaller than the cut-off value, the MCMC chains are considered to have converged. A cut-off value of 1.1 was generally recommended.[44-46]

Here, a series of computations with different numbers of samples is performed, and the corresponding PSRF values are calculated. Figure 5 shows variations of the PSRF with the number of samples, where the observed deflection at stage 3 is used as an example for updating. It is concluded that 10,000 iterations are adequate to reach a convergence state . Notably, the same convergence diagnostic is repeated for each updating stage, indicating 10,000 samples are appropriate for this case.

3.2 | Results and comparisons

Table 3 presents the model class selection results based on the observed wall deflection at stage 3. Model class 9 is the most plausible with a posterior probability of 9.27×10^{-1}, and model class 4 ranks second. Thus, the distribution pattern $D4$ is the most suitable and strut axial stiffness should be taken as an uncertain parameter in the calculations. The updated parameters of model class 9 are listed in Table 4, and the COVs of these updated parameters are computed to characterize

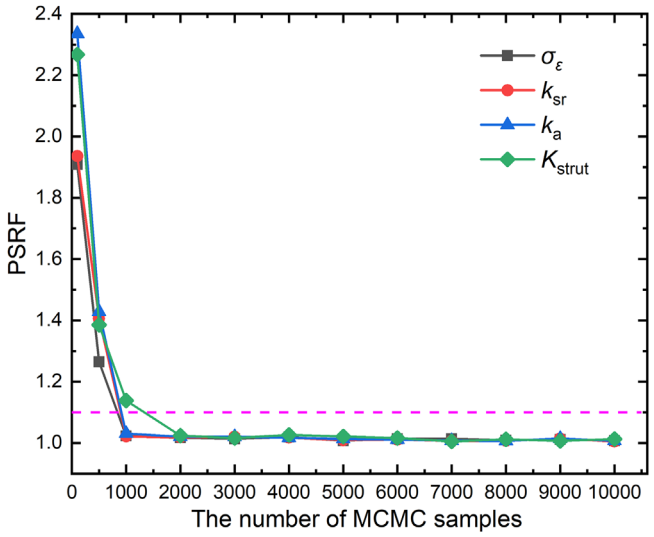

FIGURE 5 Variations of the potential scale reduction factor (PSRF) with the number of samples

TABLE 3 Model class selection results based on the observed wall deflection at stage 3

Model class number	Logarithm of evidence $ln(S)$	Posterior probability $P(M\|Y)$
1	−139.88	1.82×10^{-21}
2	−111.73	3.06×10^{-9}
3	−98.70	1.40×10^{-3}
4	−94.77	7.10×10^{-2}
5	−135.35	1.68×10^{-19}
6	−139.78	2.01×10^{-21}
7	−111.96	2.43×10^{-9}
8	−98.96	1.08×10^{-3}
9	−92.20	9.27×10^{-1}
10	−135.30	1.77×10^{-19}

TABLE 4 Posterior statistics of the updated parameters

Stage		Updated parameters			
		σ_ε (mm)	k_{sr} (kN/m^5)	k_a (kN/m^3)	K_{strut} (kN/m)
Stage 3	Mean	1.91	1.73×10^{1}	4.33	1.12×10^{5}
	COV	1.19×10^{-1}	1.00×10^{-1}	8.11×10^{-2}	2.48×10^{-1}
Stage 4	Mean	2.00	2.24×10^{1}	5.55	1.07×10^{5}
	COV	8.26×10^{-2}	7.54×10^{-2}	6.70×10^{-2}	2.24×10^{-1}
Stage 5	Mean	3.59	2.97×10^{1}	6.04	1.10×10^{5}
	COV	5.76×10^{-2}	7.35×10^{-2}	5.98×10^{-2}	1.49×10^{-1}
Stage 6	Mean	3.87	2.99×10^{1}	5.97	7.00×10^{4}
	COV	5.04×10^{-2}	7.08×10^{-2}	5.84×10^{-2}	1.47×10^{-1}

the associated uncertainties. The COVs decrease continuously as excavation proceeds, which means the uncertainties in the updated parameters are gradually reduced with the application of stage-by-stage updating.

Predictions can be made before subsequent excavation stages using the most suitable model and its updated parameters. The Monte Carlo simulation (MCS) is used to compute the deflection. The maximum deflection is analyzed first as it is one of the major references in deformation control for braced excavations.[5,6,14,37] To demonstrate the updating efficiency of the proposed method, the predictions made by the Bayesian updating framework using the KJHH model are adopted

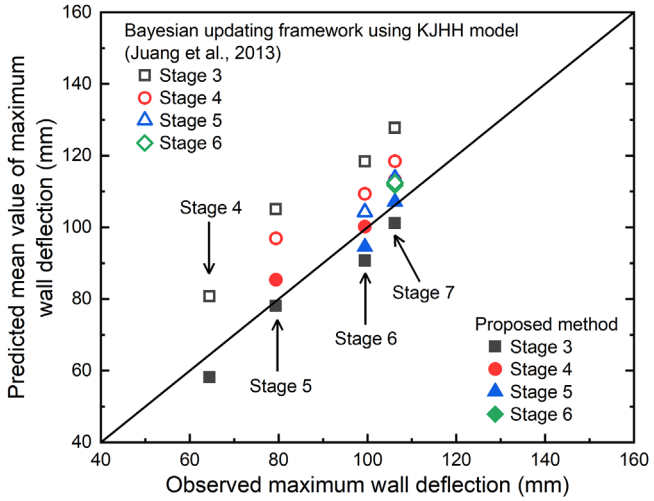

FIGURE 6 Predicted mean values of the maximum deflection versus the observed maximum deflection

for comparisons. This framework was proposed by Juang et al.,[16] where the TNEC excavation was also adopted as a case study. As described above, the KJHH model is a surrogate model of a series of well-established finite element analyses, which is very simple and computationally friendly to users as no finite element knowledge is required.[16,37] The maximum deflection and maximum settlement are outputs of the KJHH model, and two important soil parameters of the KJHH model are taken as variables and updated using field observations, which are the ratio of the average shear strength over the vertical effective stress (s_u/σ'_v) and the ratio of the average initial Young's modulus over the vertical effective stress (E_i/σ'_v).[16]

Figure 6 shows the predicted mean values of the maximum deflection versus the observations. As an example, predictions made by the Bayesian updating framework using the KJHH model at stage 3 (observations at stage 3 are used for updating), are labeled with the symbol □. These predictions are the maximum deflection of the subsequent stages (i.e., stages 4–6), which are computed using the KJHH model with the updated posterior PDFs of uncertain parameters. Although both methods can make good predictions of the maximum deflection, a more accurate assessment can be achieved by the proposed approach. Additionally, a good prediction of the maximum deflection at stage 7 can be made at stage 3 by the proposed method, whereas the KJHH-based Bayesian updating framework does not reach a comparable level of prediction accuracy until the observations in stages 3–6 are used for updating. The improved performance of the proposed method can be attributed to all the observed deflection data along the wall depth being fully used for updating, and more useful information can thusly be extracted from the observations to further improve the updating efficiency and prediction accuracy. In contrast, only information from the maximum deflection observations is used in the KJHH-based Bayesian updating framework. Notably, although two types of observations, that is, maximum deflection and maximum settlement, can be used simultaneously to update the parameters in the KJHH-based Bayesian updating framework, the amount of information provided by the observations is still limited compared with the proposed method.

Figure 7 compares the predicted and observed deflection along the wall depth. The predictions are computed using the model parameters updated with all previous data. Both the predicted magnitudes and profile of the wall deflection are in good agreement with the measurements, where the predicted error bars denote the 95% confidence interval (CI). To evaluate the prediction performance, the coefficients of determination (R^2) values for each stage are computed. The R^2 are all larger than 0.89 for the subsequent stages, indicating a remarkable ability to predict both the magnitudes and profile of wall deflection.

Previous researchers proposed an inverse analysis framework that directly combined the differential evolution algorithm and finite element modeling to predict wall deflection, with the TNEC case as an application example.[10] This study compares the performance of this inverse framework with the proposed method, with the relative error as the indicator (Figure 8).[10] The results show the prediction accuracy achieved by this study is comparable to the inverse analysis framework, and even smaller relative errors are obtained by the proposed method at the early stages. In the inverse analysis framework, finite element models involving numerous geotechnical parameters should be established, and numerous

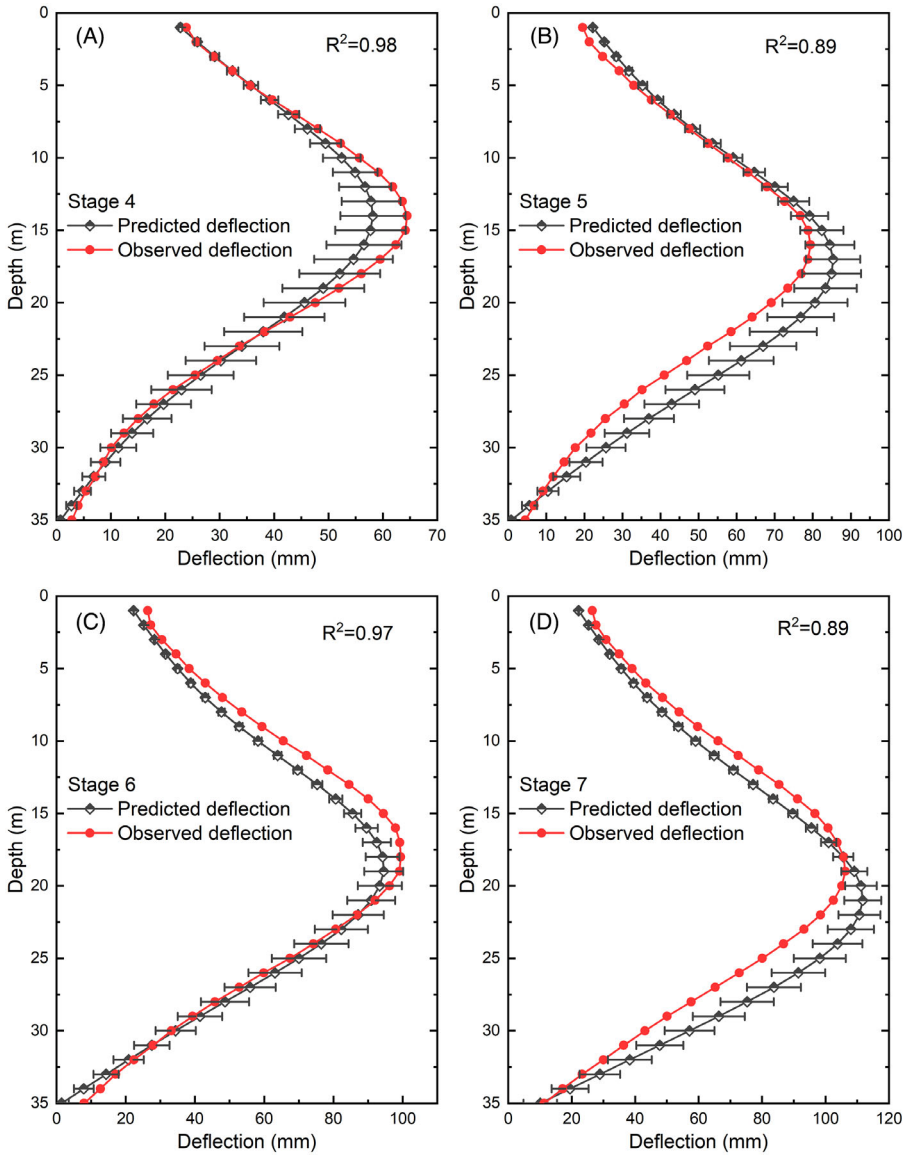

FIGURE 7 Predicted deflection (95% CI) versus observed deflection along the wall depth: (A) stage 4; (B) stage 5; (C) stage 6; (D) stage 7

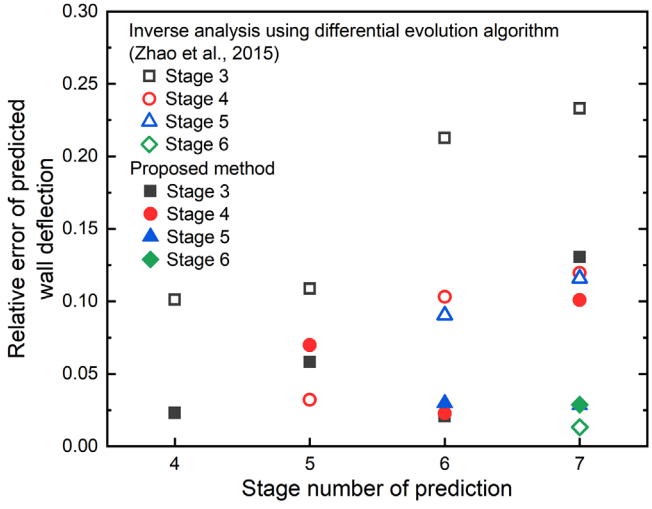

FIGURE 8 Relative prediction errors at each stage

rounds of associated computations are required. In contrast, the proposed method is more computationally friendly as no complex soil constitutive relations are involved, and uncertainty is taken into consideration.

In conclusion, there is a satisfactory agreement between the observations and predictions made using the proposed approach in this field case. Compared with the KJHH-based Bayesian updating framework, the proposed method exhibits higher updating efficiency by using all observations. An accurate prediction for the final stage can be made at the first updating stage using the proposed method, which enables an early warning and timely construction adjustments during excavations. The Bayesian updating framework using the KJHH model (or other similar surrogate models if applicable) can provide a preliminary assessment of the maximum deflection in practice as it is easier to use. The proposed method can serve as a feasible solution if more detailed predictions (i.e., for both the deflection profile and magnitudes) are required.

4 | CONCLUSIONS

This paper presents a method that combines a BEFM with a Bayesian framework for effective probabilistic predictions of wall deflection in braced excavations. A finite element solving algorithm is developed to calculate the wall deflection in the BEFM. Applications of the Bayesian method allow the determination of the most suitable distribution pattern of soil resistance and an appropriate set of uncertain parameters in the BEFM while simultaneously updating the uncertain parameters. A prediction is then made using the optimal model and its updated parameters, in which uncertainties in predictions can be estimated.

The effectiveness of predicting both the magnitudes and profile of wall deflection using the proposed method is verified by a field case study of the TNEC excavation. The proposed method is effective in model selection, parameter updating, and uncertainty quantification. Comparisons with the Bayesian updating framework using the KJHH model demonstrate the higher updating efficiency of the developed method in predicting maximum deflection as information from all observed points can be used for updating. Moreover, the performance of the proposed approach in assessing the deflection profile is demonstrated by a comparison with an inverse analysis framework that directly combined the differential evolution algorithm and finite element modeling. Results indicate remarkable prediction accuracy can be achieved by the proposed method, with R^2 values between the predictions and observations for all predicted stages larger than 0.89. Overall, the developed approach provides a valuable tool to estimate wall deflection and corresponding uncertainties along the depth with satisfactory accuracy, which is important in excavation engineering practice.

ACKNOWLEDGMENTS

The authors greatly acknowledge the financial support from the Science and Technology Development Fund, Macau SAR (File nos. 0057/2020/AGJ and SKL-IOTSC(UM)-2021-2023), the National Natural Science Foundation of China (Grant No. 52022001), the Science and Technology Program of Guangdong Province (Granted No. 2021A0505080009), and Research Committee of University of Macau (No. MYRG2018-00173-FST).

DATA AVAILABILITY STATEMENT

All the used data were cited, and the relevant references can be found in the reference list.

ORCID

Wan-Huan Zhou https://orcid.org/0000-0001-5183-9947

REFERENCES

1. Ou CY, Liao JT, Cheng WL. Building response and ground movements induced by a deep excavation. *Geotechnique*. 2000;50(3):209-220.
2. Zhang J, Xie R, Zhang H. Mechanical response analysis of the buried pipeline due to adjacent foundation pit excavation. *Tunn Undergr Space Technol*. 2018;78:135-145.
3. Zhang DM, Xie XC, Li ZL, Zhang J. Simplified analysis method for predicting the influence of deep excavation on existing tunnels. *Comput Geotech*. 2020;121:103477.
4. Shanghai Municipal Engineering Authority, Specification for excavation in Shanghai metro construction (SZ-08-2000). Tongji University Press, Shanghai; 2000.
5. Zhang WG, Goh ATC, Xuan F. A simple prediction model for wall deflection caused by braced excavation in clays. *Comput Geotech*. 2015;63:67–72.
6. Goh ATC, Zhang F, Zhang WG, Zhang YM, Liu HL. A simple estimation model for 3D braced excavation wall deflection. *Comput Geotech*. 2017;83:106–113.

7. Ren C, Liao SM, Jiao QZ, Zhang D. Deformation patterns of retaining structures in excavation and their recognition. *Chin J Geotech Eng*. 2013;35(12):2226–2232.
8. Tan Y, Jiang WZ, Luo WJ, Lu Y, Xu CJ. Longitudinal sliding event during excavation of Feng-Qi station of Hangzhou metro line 1: postfailure investigation. *J Perform Constr Facil*. 2018;32(4):04018039.
9. Hashash YMA, Levasseur S, Osouli A, Finno R, Malecot Y. Comparison of two inverse analysis techniques for learning deep excavation response. *Comput Geotech*. 2010;37:323–333.
10. Zhao BD, Zhang LL, Jeng DS, Wang JH, Chen JJ. Inverse analysis of deep excavation using differential evolution algorithm. *Int J Numer Anal Methods Geomech*. 2015;39:115–134.
11. Phoon KK, Kulhawy FH. Characterization of geotechnical variability. *Can Geotech J*. 1999;36:612–624.
12. Zhang J, Zhang LM, Tang WH. Bayesian framework for characterizing geotechnical model uncertainty. *J Geotech Geoenviron Eng*. 2009;135(7):932–940.
13. Wu SH, Ching JY, Ou CY. Probabilistic observational method for estimating wall displacements in excavations. *Can Geotech J*. 2014;51(10):1111–1122.
14. Qi XH, Zhou WH. An efficient probabilistic back-analysis method for braced excavations using wall deflection data at multiple points. *Comput Geotech*. 2017;85:186–198.
15. Sun Y, Jiang QH, Yin T, Zhou CB. A back-analysis method using an intelligent multi-objective optimization for predicting slope deformation induced by excavation. *Eng Geol*. 2018;239:214–228.
16. Juang CH, Luo Z, Atamturktur S, Huang HW. Bayesian updating of soil parameters for braced excavations using field observations. *J Geotech Geoenviron Eng*. 2013;139(3):395–406.
17. Wang L, Ravichandran N, Juang CH. Bayesian updating of KJHH model for prediction of maximum ground settlement in braced excavations using centrifuge data. *Comput Geotech*. 2012;44:1–8.
18. Zhou WH, Yuen KV, Tan F. Estimation of maximum pullout shear stress of grouted soil nails using Bayesian probabilistic approach. *Int J Geomech*. 2013;13(5): 659–664.
19. Janda T, Šejnoha M, Šejnoha J. Applying Bayesian approach to predict deformations during tunnel construction. *Int J Numer Anal Methods Geomech*. 2018;42:1765–1784.
20. Tan F, Zhou WH, Yuen KV. Effect of loading duration on uncertainty in creep analysis of clay. *Int J Numer Anal Methods Geomech*. 2018;42:235–1254.
21. Ou CY. *Deep excavation: theory and practice*. Taylor & Francis Group, London; 2006.
22. Liu GB, Wang WD. *Excavation engineering manual*. China Architecture & Building Press, Beijing;
23. Ministry of Housing and Urban-Rural Development of China, Technical specification for retaining and protection of building foundation excavations (JGJ120-2012). China Architecture & Building Press, Beijing; 2012.
24. Shanghai Municipal Commission of Housing and Urban-Rural Development, Technical code for excavation engineering (DG/TJ 08-61-2018). Tongji University Press, Shanghai; 2018.
25. Guo PP, Gong XN, Wang YX. Displacement and force analyses of braced structure of deep excavation considering unsymmetrical surcharge effect. *Comput Geotech*. 2019;113:103102.
26. Gong XN, Hou WS. *Design and construction manual for deep excavation engineering*. China Architecture & Building Press, Beijing; 2017.
27. Xu ZH, Li J, Wang WD. Back analysis of the m values in vertical elastic subgrade beam method for deep excavations. *Build Struc*. 2020;50(S1):1000–1006.
28. Li J, Cassidy MJ, Huang J, Zhang L, Kelly R. Probabilistic identification of soil stratification. *Geotechnique*. 2016;66(1):16–26.
29. Juang CH, Gong WP, Martin JR, Chen QS. Model selection in geological and geotechnical engineering in the face of uncertainty - Does a complex model always outperform a simple model? *Eng Geol*. 2018;242:184–196.
30. Reddy JN. *An introduction to the finite element method*. Mc Graw Hill, Singapore; 2006.
31. Zhou WH, Tan F, Yuen KV. Model updating and uncertainty analysis for creep behavior of soft soil. *Comput Geotech*. 2018;100:135–143.
32. Zhou WH, Yin ZY, Yuen KV. *Practice of Bayesian probability theory in geotechnical engineering*. Springer, Singapore; 2021.
33. Yuen KV. *Bayesian methods for structural dynamics and civil engineering*. John Wiley & Sons, Singapore; 2010.
34. Ching JY, Chen YC. Transitional Markov Chain Monte Carlo method for Bayesian model updating, model class selection, and model averaging. *J Eng Mech*. 2007;133(7):816–32.
35. Jin YF, Yin ZY, Zhou WH, Horpibulsuk S. Identifying parameters of advanced soil models using an enhanced Transitional Markov chainMonte Carlo method. *Acta Geotech*. 2019;14(6):1925–1947.
36. Jin YF, Yin ZY, Zhou WH, Shao JF. Bayesian model selection for sand with generalization ability evaluation. *Int J Numer Anal Methods Geomech*. 2019;43(14):2305–2327.
37. Kung GTC, Juang CH, Hsiao ECL, Hashash YMA. A simplified model for wall deflection and ground surface settlement caused by braced excavation in clays. *J Geotech Geoenviron Eng*. 2007;133(6):731–747.
38. Zheng D, Huang JS, Li DQ, Kelly R, Sloan SW. Embankment prediction using testing data and monitored behaviour: a Bayesian updating approach. *Comput Geotech*. 2018;93:150–162.
39. Ou CY, Liao JT, Lin HD. Performance of diaphragm wall constructed using top-down method. *J Geotech Geoenviron Eng*. 1998;124:798–808.
40. Jin YF, Yin ZY, Zhou WH, Huang HW. Multi-objective optimization-based updating of predictions during excavation. *Eng Appl Artif Intell*. 2019;78:102–123.
41. Harahap SE, Ou CY. Finite element analysis of time-dependent behavior in deep excavations. *Comput Geotech*. 2020;119:103300.

42. Tang YG, Kung GTC. Application of nonlinear optimization technique to back analyses of deep excavation. *Comput Geotech*. 2009;36:276–290.
43. Brooks SP, Gelman A. General methods for monitoring convergence of iterative simulations. *J Comput Graph Stat*. 1998;7(4):434–455.
44. Roy V. Convergence diagnostics for Markov chain Monte Carlo. *Annu Rev Stat Appl*. 2020;7:387–412.
45. Gelman A, Carlin JB, Stern HS, Dunson DB, Vehtari A, Rubin DB. *Bayesian data analysis*. CRC Press, Florida, USA; 2013.
46. Li ZB, Gong WP, Li TZ, Juang CH, Chen J, Wang L. Probabilistic back analysis for improved reliability of geotechnical predictions considering parameters uncertainty, model bias, and observation error. *Tunn Undergr Space Technol*. 2021;115:104051.
47. Koch MC, Osugi M, Fujisawa K, Murakami A. HamiltonianMonte Carlo for simultaneous interface and spatial field detection (HMCSISFD) and its application to a piping zone interface detection problem. *Int J Numer Anal Methods Geomech*. 2021;45:2602–2626.
48. Jin YY, Biscontin G, Gardoni P. Adaptive prediction of wall movement during excavation using Bayesian inference. *Comput Geotech*. 2021;137:104249.
49. Tang C, He SY, Zhou WH. Settlement-based framework for long-term serviceability assessment of immersed tunnels *Reliab Eng Syst Saf*. 2022;228:108801.

How to cite this article: Tang C, He S-Y, Zhou W-H. A beam on elastic foundation method for predicting deflection of braced excavations considering uncertainties. *Int J Numer Anal Methods Geomech*. 2023;47:533–548. https://doi.org/10.1002/nag.3480

APPENDIX A: DE-TMCMC ALGORITHM

The DE-TMCMC algorithm is developed based on the transitional Markov chain Monte Carlo (TMCMC) algorithm proposed by Ching and Chen.[34] The basic idea behind the TMCMC algorithm is to construct a series of intermediate PDFs that converge to the target posterior PDF from the initial prior PDF, which can be expressed as:

$$f_s(\theta) \propto f\left(\theta|\mathbf{M}^{(\mathbf{m})}\right) f\left(Y|\theta,\ \mathbf{M}^{(\mathbf{m})}\right)^{p_s}$$

$$(s = 0, 1, \ldots, N_s;\ 0 = p_0 < p_1 < \ldots < p_{N_s} = 1) \tag{A1}$$

where the subscript s signifies the stage number and N_s is the total number of stages. The intermediate PDFs enable a reasonable means of transitioning and obtaining the samples between the adjacent intermediate PDFs to avoid sampling directly from the complex target PDFs.[34] Additionally, the evidence $f(Y|M^{(m)})$ can be estimated as a by-product without additional computations.

To overcome possible local convergence, Jin et al.[35,36] proposed the DE-TMCMC algorithm by integrating the differential evolution technique into the TMCMC algorithm, whose capabilities in model selection and parameter updating are verified through a series of case studies.[35,36] Thus, the DE-TMCMC algorithm is adopted to perform effective sampling in the complex calculations of the BEFM. The modified algorithm can be enacted in the following steps:

(1) At the initial stage ($s = 0$), generate samples $\{\theta_{0,k} : k = 1, 2, \cdots, N_0\}$ from the prior PDF $f_0(\theta)$.
(2) Compute the plausibility weight $w(\theta_{s,k}) = f(Y|\theta_{s,k},\ M^{(m)})^{p_{s+1}-p_s}$ for $k = 1, 2, \ldots, N_s$, and choose p_{s+1} by comparing the COV of $w(\theta_{s,k})$ with a prescribed threshold. Here, $\theta_{s,k}$ denotes the kth sample that belongs to stage s.
(3) Compute the weighting coefficient $S_s = \sum_{k=1}^{N_s} w(\theta_{s,k})/N_s$, which is used to compute the evidence $f(Y|M^{(m)})$ hereafter.
(4) Select the resampling index l from the set $[1, 2, \ldots, N_s]$ using the sequential importance sampling (SIS) method, where each l is assigned a probability $w(\theta_{s,k})/\sum_{l=1}^{N_s} w(\theta_{s,k})$.
(5) Generate the new samples from Equations (A2) and (A3), while the Metropolis-Hastings (MH) algorithm is employed to judge whether to accept these new samples,

$$\theta_{s,l}^{\text{new}} = \theta_{s,l}^{\text{c}} + d\theta_{s,l} \tag{A2}$$

with

$$d\,\theta_{s,l} = (1+\lambda)\gamma\left[\left(\theta_s^{\text{best}} - \theta_{s,l}^{\text{c}}\right) + \left(\theta_{s,a} - \theta_{s,b}\right)\right] + \zeta \tag{A3}$$

where $\theta_{s,l}^{\text{new}}$ is the new sample, $\theta_{s,l}^{\text{c}}$ is the current sample, $d\theta_{s,l}$ is the jump between the new sample and current sample, and θ_s^{best} is the sample corresponding to the maximum weight in the current iteration. More details about Equation (A3) can be found in Jin et al.[35,36]

Steps (2)–(5) are repeated until level N_s has been reached, that is, $p_{N_s} = 1$. At this stage, samples $\{\theta_{N_s,k} : k = 1, 2, \cdots, N_{N_s}\}$ are asymptotically distributed as $f(\theta|\mathbf{Y}, \mathbf{M}^{(\mathbf{m})})$, and $S = \prod_{s=0}^{N_s-1} S_s$ is an asymptotically unbiased estimation of the evidence $f(Y|M^{(m)})$.[34] This procedure is repeated for all model classes $\{M^{(m)} : m = 1, \ldots, N_m\}$ to obtain corresponding evidence $S^{(m)}$, after which the model class selection is performed using Equation ([13]).